3-Dimensional Localization via RFID Tag Array

Yuan Zhang[†], Lei Xie[†], Yanling Bu[†], Yanan Wang[†], Jie Wu[‡], and Sanglu Lu[†]
[†]State Key Laboratory for Novel Software Technology, Nanjing University, China
[‡]Center for Networked Computing, Temple University, USA
Email: zhangyuan@smail.nju.edu.cn, lxie@nju.edu.cn, {yanling,yananwang}@smail.nju.edu.cn,
jiewu@temple.edu, sanglu@nju.edu.cn

Abstract—In this paper, we propose *3DLoc*, which performs 3-dimensional localization on the tagged objects by using the RFID tag arrays. *3DLoc* deploys three arrays of RFID tags on three mutually orthogonal surfaces of each object. When performing 3D localization, *3DLoc* continuously moves the RFID antenna and scans the tagged objects in a 2-dimensional space right in front of the tagged objects. It then estimates the object's 3D position according to the phases from the tag arrays. By referring to the fixed layout of the tag array, we use Angle of Arrival-based schemes to accurately estimate the tagged objects' orientation and 3D coordinates in the 3D space. To suppress the localization errors caused by the multipath effect, we use the linear relationship of the AoA parameters to remove the unexpected outliers from the estimated results. We have implemented a prototype system and evaluated the actual performance in the real complex environment. The experimental results show that *3DLoc* achieves the mean accuracy of 10cm in free space and 15.3cm in the multipath environment for the tagged object.

I. INTRODUCTION

A. Motivation

Nowadays, RFID has been widely used in several applications such as warehouse and logistic management. In these applications, each of the items is attached with one or more RFID tags, which illustrate the detailed information of the specified items, e.g., the production/expiration dates, manufacturers, etc. With the assistance of RFID, many novel functions such as indoor localization can be effectively realized. For example, with the exact locations of all items on the shelves, the robotic arm can be used to fetch the specified items in a fully automated manner. However, most state-of-art RFID-based localization schemes, such as PinIt [10] and Tagoram [12], mainly focus on the localization in the 2-dimensional(2D) space, e.g., they usually provide the 2D coordinates of the objects in the indoor maps. These solutions usually fail to locate the items which are arbitrarily stacked in the 3-dimensional(3D) space, as shown in Fig. 1. Therefore, it is essential to propose an RFID-based mechanism to accurately perform 3D localization, so that the 3D coordinates of the objects can be figured out in the 3D space.

B. Proposed Approach

In this paper, we propose *3DLoc*, which performs 3D localization on the tagged objects by using the RFID tag arrays. The basic idea is as follows: Without loss of generality, we assume that the tagged object is a cuboid with six surfaces, e.g., an express package or a cardboard box. For each of the specified objects, three arrays of RFID tags are attached onto three mutually orthogonal surfaces of the object in advance.

Fig. 1. Illustration of *3DLoc*

When performing the 3D localization, the RFID antenna continuously moves and scans the tagged objects in a 2D space right in front of the tagged objects. Specifically, the RFID antenna first moves along the Z axis and scans all tags to estimate the Z-coordinate of each tag from the tag array, *3DLoc* then estimates the rough orientation of the object and selects a target tag array for further localization in the X-Y plane. After that, the RFID antenna moves along the X axis and scans the tags in the target tag array. As it obtains the phase values from the tag arrays, it estimates the object's orientation and figures out the object's 3D coordinates in the 3D space, by leveraging the *Angle of Arrival*(AoA)-based localization schemes. For the layout of the tag array, each tag's ID and relative position are known in advance to support the 3D localization.

C. Challenges and Solutions

There are two technical challenges in realizing 3D localization for the tagged objects. First, the 3D localization results can be severely impacted by interferences such as the multipath effect from the indoor environment. Due to the continuously changing factors in the multipath effect, it distorts the phase values of tags in a very unpredictable approach, thus it could further lead to errors in the AoA-based localization. To address this challenge, we perform mobile scanning to continuously sample the phases of the specified tags at different positions, compute the spatial angles of arrival of the tags in different locations, and suppress the outliers caused by the multipath effect. By using the mobile scanning-based scheme, *3DLoc* investigates and uses the linear relationship of the AoA parameters to remove the unexpected outliers from the estimated results via continuous sampling, so it is robust to the interferences including ambient noises and the multipath effect.

Second, the orientation of the tagged objects is essential to be firstly determined before performing accurate 3D localiza-

tion for the tagged objects. However, according to the phase values from one tag array, it is usually difficult to completely determine the exact orientation of the tagged objects, as there exist multiple possibilities of the orientation state in the 3D space. To address this challenge, we attach three tag arrays to three mutually orthogonal surfaces of the object, respectively. By comparing the AoA parameters from multiple tag arrays, *3DLoc* is able to accurately estimate the orientation of the tagged object. We then select a target tag array vertically deployed on the vertical plane, and further figure out the 3D position of the specified object.

D. Contributions

To the best of our knowledge, this is the first work to consider 3D-localization of tagged objects by using the RFID tag arrays. We make three contributions in this paper. 1) To perform accurate 3D localization for the tagged objects, we deploy tag arrays on three mutually orthogonal surfaces of the object. By referring to the fixed layout of the tag array, we use the AoA-based schemes to accurately estimate the tagged object's orientation and 3D coordinates in the 3D space. 2) To suppress the localization errors caused by the multipath effect, we propose a mobile scanning-based scheme and use the linear relationship of the AoA parameters to remove the unexpected outliers from the estimated results via continuous sampling. 3) We have implemented a prototype system with the COTS RFID system, and evaluated the actual performance in the real complex environment. The experimental results show that *3DLoc* achieves the mean accuracy of 10cm in the free space and 15.3cm in the multipath environment for the tagged object.

II. RELATED WORK

Many approaches have been proposed in RFID localization system. RSSI information is widely used for localization [1–5], but it is limited for accurate absolute localization since RSSI-based approaches are not sensitive enough to distance change. Different from RSSI, the tag's phase value is distance sensitive: the phase difference obtained at two antenna positions reflects different distances from the tag to the corresponding antenna position. Current RF-based localization solutions have great interest in using the phase values to locate the tagged objects, and they mainly fall into distance-based methods [6–8], AoA-based methods [9–11], and holography-based methods [12, 13]. For example, BackPos [7] infers the distance difference from the phases detected by antennas, and uses a hyperbolic-based method for localization. RF-IDraw [11] leverages the phase differences as well, but it uses an AoA-based method to reconstruct the gestures of a user. Tagoram [12] uses the holography-based method to calculate the possibility of each point being the RF source in the 2D surveillance plane and selects the most likely position as the tag's location. These above solutions only address the 2D localization problem, but fail to provide 3D coordinates of the objects. *3DLoc* creatively proposes a 3D localization approach: it estimates the rough orientation of the object first, then calculates the location of the object from the phases of the tags in the target tag array.

Meanwhile, in the indoor environment, the wireless signals suffer from multipath propagations which will distort the phase values and lead to errors in the localization results. Many researches have focused on suppressing the negative impacts caused by the multipath [10, 13]. PinIt [10] deploys many reference tags in advance and exploits the similar multipath profiles of the nearby RFIDs which experience a similar multipath environment to pinpoint a tag's location. MobiTagbot [13] leverages the changing carrier frequency of the RFID query to detect whether the phase value is obtained in severe multipath location, and only uses the phases obtained in low multipath locations for further localization. Similar to MobiTagbot, *3DLoc* uses the linear relationship of the AoA parameters to find and remove the unexpected outliers which result from multipath effect. What's more, instead of localizing each tag respectively as prior solutions, *3DLoc* views the tags in the tag array as a whole, and designs a novel algorithm to calibrate each tag's position referring to the fixed layout of the tag array and finally estimate the location and orientation of the tagged object.

III. MODELING THE 3D LOCALIZATION

A. AoA-based Localization

The phase value is a common metric in the RFID localization system. It reflects the phase rotation between the tag's backscattered signal and the signal sent by the antenna. Let d be the distance between the tag and the reader antenna, then the backscattered signal traverse a round trip of $2d$. Besides the phase rotation over distance, the antenna's transceiver and the tag's reflection characteristic will also introduce additional phase rotations, denoted as ϕ_A and ϕ_T, respectively. Hence, the total phase rotation ϕ can be expressed as:

$$\phi = \left(2\pi \cdot \frac{2d}{\lambda} + \phi_A + \phi_T\right) \mod 2\pi \qquad (1)$$

In an RF localizing system, phases obtained at different positions are related to the tag's angles of arrival for the antenna at different positions. As illustrated in Fig.2, the antenna interrogates a tag at two different positions x_1 and x_2, with phase readings ϕ_1 and ϕ_2. The distances from the tag to x_1 and x_2 are d_1 and d_2, and Δx is the distance of $|x_1 x_2|$. According to Eq.1, for the same tag and the same antenna, ϕ_1 and ϕ_2 share the same ϕ_A and ϕ_T, thus the phase difference $\Delta \phi_{1,2} = \phi_1 - \phi_2$ is related to the distance difference $\Delta d_{1,2} = d_1 - d_2$, as:

$$\Delta \phi_{1,2} = 2\pi \cdot \frac{2\Delta d_{1,2}}{\lambda} + 2k\pi \qquad (2)$$

where k is an integer which ensures that $\Delta \phi_{1,2}$ is within the range $[0, 2\pi]$. As can be seen from Fig.2, when the tag is relatively far from the antenna, $\Delta d_{1,2} \approx \Delta x \cdot \cos\theta$, where θ is the angle of arrival of the tag at x (the midpoint of $x_1 x_2$). Combined with Eq.2, $\cos\theta$ can be expressed as:

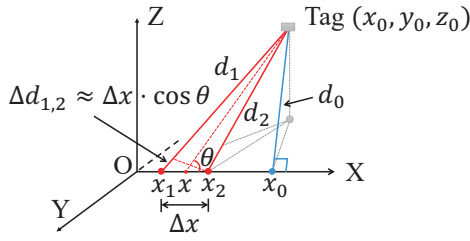$$\cos\theta = \frac{\lambda(\Delta\phi_{1,2} - 2k\pi)}{4\pi\Delta x}$$

Fig. 2. The angle of arrival of the tag

(a) Free space

(b) Severe multipath

Fig. 3. Comparisons of $\left(\tilde{x}_i, \cot \tilde{\theta}_i\right)$ in two cases

If we set Δx to be no greater than $\lambda/4$, then k must equal 0 to ensure $-1 \leq \cos \theta \leq 1$, hence θ is unique. Therefore, we can get the angle of arrival θ of the tag at position x as follows:

$$\begin{cases} \theta = \arccos \left(\dfrac{\lambda \cdot \Delta \phi_{1,2}}{4\pi \Delta x} \right) \\ x = \dfrac{x_1 + x_2}{2} \end{cases} \tag{3}$$

In conclusion, based on two phase readings obtained by the antenna at different positions, we can calculate the angle of arrival of the tag at the corresponding position.

*B. AoA Localization via Mobile Scanning*

Due to ambient noises and the multipath effect from the environment, the phase values of the tag will be distorted, which will lead to errors in the AoA-based localization. Therefore, we perform mobile scanning to continuously obtain the phases of the tag at different positions, from which we can calculate the spatial angle of arrival of the tag when the antenna is at different positions and use the linear relationship of the AoA parameters to estimate the location of the tag. In the 3D space, we assume that the antenna moves at a constant speed v along a certain line. Without loss of generality, suppose the X axis is along the antenna's moving trajectory. Then, the position of the antenna $x(t)$ at time t can be inferred by:

$$x(t) = x(t_0) + v \cdot (t - t_0)$$

where t_0 is the start time and $x(t_0)$ is the initial position of the antenna. Let $\mathbf{X} = \{x(t_0), x(t_1), \cdots, x(t_n)\}$ be the antenna's positions at different interrogated time, where $x(t_i)$ is the ith antenna's position at interrogated time t_i. We define $\phi(t_i)$ as the phase value from the antenna at $x(t_i)$, so the phase measurements can be denoted as $\mathbf{\Phi} = \{\phi(t_0), \phi(t_1), \cdots, \phi(t_n)\}$. Recall that based on two phase readings at different positions, the spatial angle of arrival of the tag can be calculated. So, we can choose phase tuples from $\mathbf{\Phi}$ for the estimation of angles of arrival, denoted as $\mathbf{T} = \{\langle \phi(t_0), \phi(t_{k_0}) \rangle, \langle \phi(t_1), \phi(t_{k_1}) \rangle, \cdots, \langle \phi(t_m), \phi(t_{k_m}) \rangle\}$. For each tuple $\langle \phi(t_i), \phi(t_{k_i}) \rangle$, $0 \leq i < k_i \leq n$, and the distance Δx_i between two antenna locations $x(t_i)$ and $x(t_{k_i})$ should meet the following condition:

$$\Delta x_i = x(t_{k_i}) - x(t_i) \leq \lambda/4$$

Based on each tuple in $\mathbf{T}$, we can calculate the angle of arrival of the tag when the antenna is at different positions according to Eq.3, the results can be denoted as $\mathbf{R} = \left\{ \left(\tilde{x}_0, \tilde{\theta}_0\right), \cdots, \left(\tilde{x}_m, \tilde{\theta}_m\right) \right\}$. Then the location of the tag can
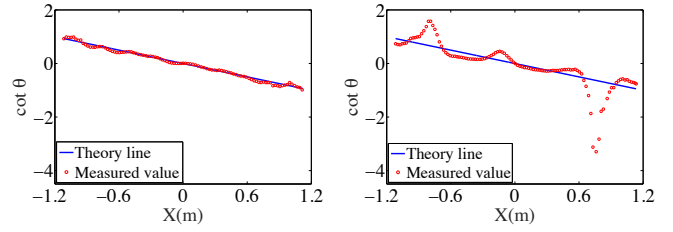
be estimated relying on the linear relationship of the AoA parameters in $\mathbf{R}$ as described in *Theorem 1*.

Theorem 1: Let the antenna's linear moving trajectory be the X axis and θ be the angle of arrival of the tag at position x, then $\cot \theta$ and x and have the following linear relationship:

$$\cot \theta = -\frac{1}{d_0} (x - x_0) \tag{4}$$

where d_0 is the vertical distance from the tag to the X axis and x_0 is the X-coordinate of the tag.

Proof: As illustrated in Fig.2, according to the triangle relationship, we have:

$$x_0 - x = d_0 \cdot \cot \theta$$

from which we can easily infer Eq.4. Then the slope of the line equals $-1/d_0$, and x_0 equals the X-intercept of the line, because at position x_0, θ equals $\pi/2$, then $\cot \theta = 0$. ∎

Therefore, with the angle of arrival result set $\mathbf{R}$, we replace θ with $\cot \theta$, then the transformed result set is $\mathbf{P} = \left\{ \left(\tilde{x}_0, \cot \tilde{\theta}_0\right), \cdots, \left(\tilde{x}_m, \cot \tilde{\theta}_m\right) \right\}$, and the points in $\mathbf{P}$ should form a line as described in Eq.4. To validate the above theorem, we conduct empirical studies using a COTS RFID platform in both free space and the severe multipath environment. The antenna is programmed to move at a constant speed of 15cm/s along a linear trajectory, and the tag's vertical distance to the trajectory is 1.2m. We plot the $x - \cot \theta$ diagram along with the theory line calculated by Eq.4 in Fig.3.

1) Free space: As shown in Fig.3(a), all points fit well with the theory line. Specifically, we can use the *linear least squares* to find a fitting line for the calculated points to estimate d_0 and x_0 based on Eq.4.

2) Multipath environment: In the severe multipath scenario, as shown in Fig.3(b), we make the following observation:

Observation 1 *There are many outliers away from the theory line and the occurrence of them is continuous.*

Intuitively, for the outliers, we can infer that errors exist in their angles of arrival results. Since the angle of arrival of the tag is calculated from the phase values of the tag, in a multipath environment, the backscattered signal from the tag will bounce off objects like walls and the ground, thus the phase readings are not only related to the signal that propagates along the direct path, but also related to the unpredictable signals that reflect from other objects. Recall that based on the phase tuple $\langle \phi(t_i), \phi(t_{k_i}) \rangle$, we can compute the tag's spatial angle of arrival $\tilde{\theta}_i$ and corresponding coordinates
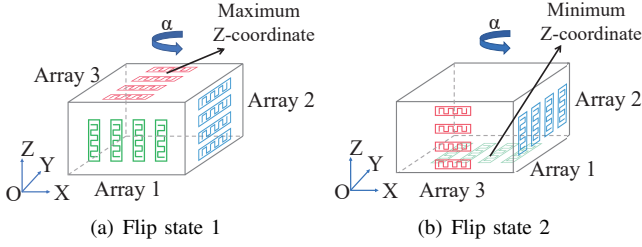
(a) Flip state 1   (b) Flip state 2

Fig. 4.   Flip of the object

Fig. 5.   Rotation angle of the tagged object: It is defined as the angle between X axis and the vector which points from the 1st tag to the nth tag in the target tag array

(a) $0 \leq \alpha < \frac{\pi}{2}$ (b) $\frac{\pi}{2} \leq \alpha < \pi$

(c) $\pi \leq \alpha < \frac{3\pi}{2}$ (d) $\frac{3\pi}{2} \leq \alpha < 2\pi$

Fig. 6.   Four cases for the rotation angle

$\tilde{x}_i$ in the antenna's trajectory, denoted as $\left(\tilde{x}_i, \tilde{\theta}_i\right)$. If both $\phi(t_i)$ and $\phi(t_{k_i})$ are obtained in the free space, the point $\left(\tilde{x}_i, \cot \tilde{\theta}_i\right)$ should be on the theory line according to Theorem 1. However, if either one of the phase readings suffers from severe multipath, the accuracy of $\tilde{\theta}_i$ will be impacted, so the point $\left(\tilde{x}_i, \cot \tilde{\theta}_i\right)$ will be far away from the line and can be considered as an *outlier*. Also, the occurrence of the outliers is *continuous*. This is because if we find that one certain antenna's position suffers from the severe multipath, then the nearby positions can be inferred to be affected by multipath effect at different extents.

C. Tag Array-based Localization

To localize the tags on the object, the orientation of the tagged objects needs to be firstly determined so as to perform the accurate 3D localization for the tagged objects. However, it is not enough to use a single tag to perform accurate localization as there exist multiple possible orientation states for the object in the 3D space. Thus we deploy RFID tag arrays on the three mutually orthogonal surfaces of the object and the three tag arrays are along mutually orthogonal directions. First, we specify a 3D coordinate system for the antenna: the X axis is along the antenna's moving direction and the X-Y plane is parallel to the ground. Specifically, we use two kinds of motions to describe the orientation of the tagged object in the 3D space. First, the object turns over in the 3D space, resulting in different surfaces touching the ground. We define this kind of motion as a *flip*. Second, the object *rotates* along the Z axis.

1) Flip State: Fig.4 shows two flip states of a tagged object. The surface deployed Array 1 faces towards us in Fig.4(a), when the object flips, it is on the ground (Fig.4(b)). Different flip states result in different layouts for the three tag arrays. No matter how the object flips, there always exists a certain tag array which is on the top/bottom surface of the object. Therefore, the flip state of the object can be inferred with the tag array which is on the top/bottom surface.

Notice that the Z-coordinates of the tags in the three tag arrays have different characteristics. The tags in the tag array which is on the top/bottom surface (i.e. Array 3 in Fig.4(a)) have the same Z-coordinate value and the value is the maximum/minimum. For the other two tag arrays which are on the two vertical surfaces, the directions of the tags in the two tag arrays are different. For the tag array in which each tag is along the Z axis (i.e. Array 1 in Fig.4(a)), the tags also have the same Z-coordinate. For the last tag array (i.e. Array 2 in Fig.4(a)), the tags have different Z-coordinates. In
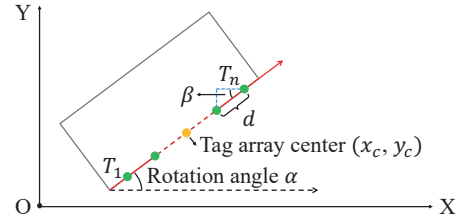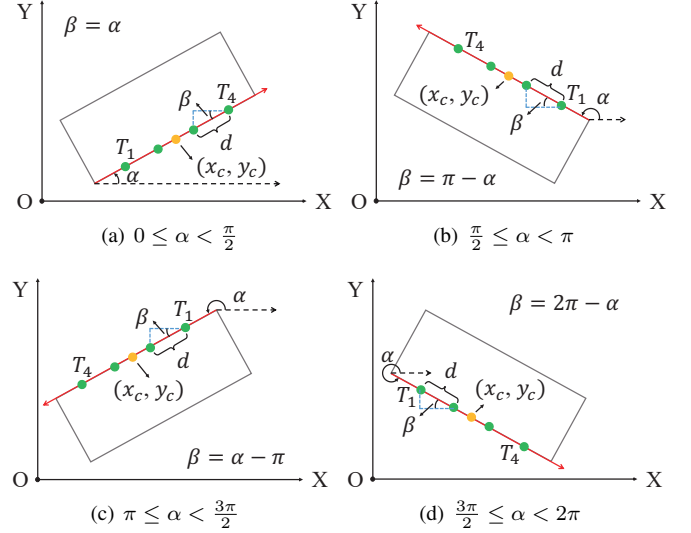
practice, we move the antenna along the Z axis to estimate the Z-coordinates of all the tags in the three tag arrays. By comparing the Z-coordinate of each tag array, we can infer how the object flips and distinguish the three tag arrays on the different surfaces.

2) Rotation angle: To estimate the rotation angle of the object, we can project the rotation of the object onto the X-Y plane. Taking Fig.4(a) for example, the tags in Array 2 have the same X-coordinate and Y-coordinate and their projections become a same point in the X-Y plane, thus it is infeasible to use Array 2 to estimate the rotation angle. Both Array 1 and Array 2 can be used for rotation angle estimation and in this paper, we choose the tag array in which each tag is along the Z axis(Array 1 in Fig 4(a)) as the *target tag array* for the rotation angle estimation and further localization in the X-Y plane. Suppose the target tag array is composed of n tags, and for brevity, we consider the distance between two adjacent tags to be the same, termed as d.

As illustrated in Fig.5, the rotation of the object and the *target tag array* are projected onto the X-Y plane. We define the rotation angle of the object as the angle between the X axis and the vector which points from the 1st tag to the nth tag. Let (x_c, y_c) be the coordinates of the tag array's center in the X-Y plane and α be the rotation angle of the object, where α is in the range $[0, 2\pi]$. Obviously, (x_c, y_c) and α can uniquely determine the target tag array's position in the X-Y plane.
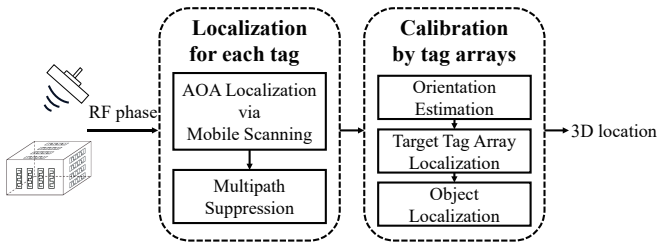
The relative position of the tags in the target tag array

Fig. 7. System architecture

changes as the object rotates. Taking the four-tag linear array for example, as illustrated in Fig.6, we divide α in four cases. For each case, the four tags in the tag array have different relative positions in the X and Y axes. Once we identify which case α belongs to, the relative layout of the four tags in the X and Y axis is uniquely determined. Then, the coordinates of the four tags can be expressed as a function of x_c, y_c and α, i.e. in Fig.6(b), $\pi/2 \leq \alpha < \pi$, and for T_1, we have:

$$\begin{cases} x_1 = x_c + \dfrac{3}{2}d\cos\beta \\ y_1 = y_c - \dfrac{3}{2}d\sin\beta \\ \beta = \pi - \alpha \end{cases}$$

More generally, for the ith tag in the n-tag tag array, its coordinates (x_i, y_i) can be expressed as:

$$\begin{cases} x_i = x_c + p_i \cdot d\cos\beta \\ y_i = y_c + q_i \cdot d\sin\beta \\ \beta = f(\alpha) \end{cases} \qquad (5)$$

where $|p_i|$ and $|q_i|$ are related to the number of tags in the target tag array, and $f(\alpha)$ is determined by the case that α belongs to as shown in Fig.6. Thus, (x_c, y_c) and α can be estimated by each tag's coordinate (x_i, y_i). In practice, we move the antenna along the X axis to calculate the coordinates of all the tags in the target tag array, then calibrate the calculated results of each tag to localize the target tag array and compute the rotation angle of the object.

IV. SYSTEM DESIGN

A. System Overview

3DLoc is a 3D localization system for the tagged object using tag arrays, as illustrated in Fig.7, it involves two main components.

1) Localization for each tag: We move the RFID antenna in a 2-dimensional space continuously to interrogate all the tags on the tagged object and localize each tag using an Angle of Arrival(AoA)-based scheme. To weaken the negative impact of multipath, we adopt a multipath suppression algorithm to optimize the localization results.

2) Calibration by tag array: We consider all the tags in the tag array as whole and by referring to the fixed layout of the tag array, the location of each tag can be calibrated and we can calculate the object's 3D location. Specifically, we first estimate the object's rough orientation and then select a target tag array for further localization of the object.

B. Localization for each tag

1) AoA Localization via Mobile Scanning: To perform 3D localization for the object, we move the antenna in a 2D space along two different axes. Without loss of generality, we will discuss our approach assuming that the antenna moves along the X axis. As aforementioned, when the antenna interrogates the tag at different positions along the X axis, we can calculate the tag's angles of arrival in different locations and denote the results as $\mathbf{R} = \left\{ \left(\tilde{x}_0, \tilde{\theta}_0\right), \cdots, \left(\tilde{x}_m, \tilde{\theta}_m\right) \right\}$. According to Theorem 1, x and $\cot\theta$ are of a linear relationship, and the line can be described as a function of x_0 and d_0 according to Eq.4 as:

$$\cot\theta = -\frac{1}{d_0}(x - x_0)$$

where d_0 is the vertical distance from the tag to the X axis and x_0 is the X coordinate of the tag. Hence with the point set $\mathbf{P} = \left\{ \left(\tilde{x}_0, \cot\tilde{\theta}_0\right), \cdots, \left(\tilde{x}_m, \cot\tilde{\theta}_m\right) \right\}$, we adopt the *linear least squares* in order to find a fitting line that best fits all these points to estimate d_0 and x_0, The objective function is formalized as follows:

$$\arg\min_{d_0, x_0} \sum_{i=0}^{m} \left| \left(-\frac{1}{d_0} \cdot (\tilde{x}_i - x_0)\right) - \cot\tilde{\theta}_i \right|^2 \qquad (6)$$

Subject to:

$$\mathbf{P} = \left\{ \left(\tilde{x}_0, \cot\tilde{\theta}_0\right), \cdots, \left(\tilde{x}_m, \cot\tilde{\theta}_m\right) \right\}$$

2) Multipath Suppression: In the multipath environment, according to Observation 1, there exist continuous occurrences of outliers in the point set $\mathbf{P} = \left\{ \left(\tilde{x}_0, \cot\tilde{\theta}_0\right), \cdots, \left(\tilde{x}_m, \cot\tilde{\theta}_m\right) \right\}$. Obviously, the outliers will definitely influence the result of the fitting line for the point set $\mathbf{P}$, thus the accuracies of d_0 and x_0 will be degraded. So, the basic idea of our multipath suppression algorithm is to find and remove the outliers from the point set $\mathbf{P}$. As shown in Fig.8, since the occurrence of the outliers is continuous, we use a slide window to split the point set $\mathbf{P}$ into k subsets: $\mathbf{S}_P = \{S_{P_1}, \cdots, S_{P_k}\}$, where S_{P_i} is i^{th} subset from $\mathbf{P}$, and the window size is a predefined value w. We denote the ground truth line for $\mathbf{P}$ as l. Intuitively, if S_{P_i} does not contain continuous occurrence of the outliers, $\cot\theta$ will change linearly with x and the average *changing rate* of the points in S_{P_i} can be regarded as the scope of l. On the contrary, if the outliers continuously occur in S_{P_i}, $\cot\theta$ will change irregularly with x and its average changing rate cannot be considered as the scope of l.

How can we evaluate the changing rate for each subset? In practice, for each subset S_{P_i} in $\mathbf{S}_P$, we use the *linear least squares* to find a fitting line l_i for all the points in S_{P_i}. Let a_i be the scope of l_i, then a_i can be considered as the average changing rate for the points in S_{P_i}. Finally we will get a changing rate set $\mathbf{A} = \{a_1, \cdots, a_k\}$ for k subsets in $\mathbf{S}_P$. In theory, except for those subsets which contain continuous occurrences of outliers, the other changing rate values in $\mathbf{A}$ should be close to the scope of l. Based on the
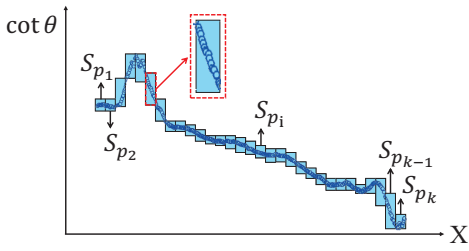
Fig. 8. Segmentation for the points in **P**

Algorithm 1: Multipath Suppression

Input: Point set $\mathbf{P} = \left\{ \left(\tilde{x}_0, \cot \tilde{\theta}_0 \right), \cdots, \left(\tilde{x}_m, \cot \tilde{\theta}_m \right) \right\}$

Output: New point set $\mathbf{P}'$ removed the outliers

1 Split $\mathbf{P}$ into k subset using a slide window:
$\mathbf{S}_P = \{ S_{P_1}, \cdots, S_{P_k} \}$;

2 Changing rate set for the subsets: $\mathbf{A} = \emptyset$;

3 **Calculation for average changing rate step:**

4 **for** *each S_{P_i} in $\mathbf{S}_P$* **do**

5 | Calculate a fitting line l_i for the points in S_{P_i} ;

6 | Add the scope a_i of l_i to $\mathbf{A}$;

7 $\mathbf{A} = \{ a_1, \cdots, a_k \}$;

8 **Outliers finding and removing step:**

9 Find outliers in $\mathbf{A}$ and remove the points in corresponding subsets in $\mathbf{S}_P$;

10 **for** *each subset which has been removed* **do**

11 | **if** *S_{P_j} and $S_{P_{j+2}}$ are removed* **then**

12 | | Remove $S_{P_{j+1}}$ if it has not been removed;

13 **return** a new point set $\mathbf{P}'$

---

above idea, we only need to find the outliers in $\mathbf{A}$ and remove the corresponding subsets in $\mathbf{S}_P$, and the above finding process can be considered as a one class SVM problem. After the above step, the subsets which contain continuous occurrences of outliers are partly removed. We can further remove the other unexpected subsets in $\mathbf{S}_P$ using the continuity of the outliers again. That is to say, if the subsets S_{P_j} and $S_{P_{j+2}}$ are removed, then the subset $S_{P_{j+1}}$ should be removed too. As a result, we removed the outliers in $\mathbf{P}$ for the estimation of d_0 and x_0. The multipath suppression algorithm is shown in Algorithm 1.

C. Calibration by tag arrays

After the AoA localization for each tag in the tag array, we can leverage the fixed layout of the tag array to calibrate the result of each tag in order to estimate the 3D coordinates and orientation of the object. In general, this part includes three main components: first, we use the calculated Z-coordinates of all the tags to infer the rough orientation of the object, from which we *distinguish* the three tag arrays on different surfaces and *select* a *target tag array* for further localization in the X-Y plane. Then, we localize the target tag array in the X-Y plane and estimate the rotation angle of the object. Finally, we get the 3D coordinates of the object referring to the location of the target tag array and the rotation angle of the object. The

---

Algorithm 2: Calibration by tag arrays

1 **Orientation Estimation:**

2 The antenna moves along the Z axis to estimate the Z-coordinates of the all the tags;

3 Distinguish the three tag arrays on different surfaces;

4 Judge the flip state of the object by finding the tag array which is on the bottom/top surface;

5 Select the target tag array and calibrate the Z-coordinate of the target tag array according to Eq.7;

6 **Target Tag Array Localization:**

7 The antenna moves along the X axis to localize the tags in the target tag array in the X-Y plane;

8 Calculate the location of the target tag array and estimate the rotation angle of the object according to Eq.8;

9 **Object Localization:**

10 Calculate the 3D coordinates of the object based on the location of the target tag array and the rotation angle of the object according to Eq.9;

11 **return** 3D coordinates of the object

---

whole algorithm is described in Algorithm 2.

1) Orientation Estimation: The orientation of the tagged objects must be firstly determined before performing an accurate 3D localization for the tagged objects. First, we need to distinguish the tag arrays on three mutually orthogonal surfaces. Recall that the Z-coordinates of the tags in the three tag arrays have different characteristics. In practice, we first move the antenna along the Z axis to estimate the Z-coordinates of all the tags, then the three tag arrays can be distinguished by comparing the Z-coordinate of each tag in the tag arrays. As illustrated in Fig.9(a), the antenna moves along the Z axis to calculate the Z-coordinate of the all the tags. Fig.9(b) shows the localization results. Notice that the Z-coordinates of the tags in Array 1 and Array 2 are equal and in Array 3 are different, so we can easily correspond the red points in Figure.9(b) to Array 3. Since the tag array on the top/bottom surface has the maximum or the minimum Z-coordinate value, so, the green points with the minimum Z-coordinates in Fig.9(b) correspond to Array 1 and we can also infer that Array 1 is at the bottom. Finally, the blue points corresponds to Array 2. After the above process, the flip state of the object is figured out. In addition, as mentioned before, the rotation angle of the object can be estimated from the target tag array in which every tag is attached along the Z axis and on the vertical surface of the object, so here Array 2 can be chosen as the target tag array.

We next optimize the Z-coordinate of the target tag array. Let z_c be the Z-coordinate of the target tag array's center and $\widehat{z}_i$ be the Z-coordinate for the ith tag calculated through AoA localization. As the Z-coordinate of each tag in the target tag array is the same, then, z_c can be considered as the average Z-coordinate of all the tags in the target tag array:
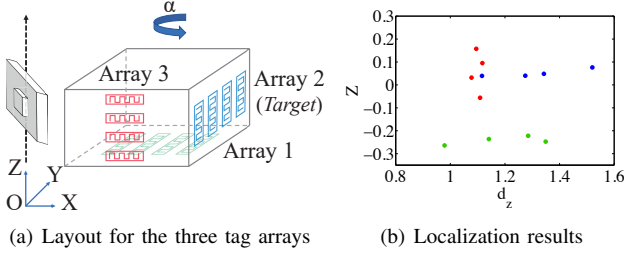
$$z_c = \frac{\sum_{i=1}^{n} \widehat{z}_i}{n} \tag{7}$$

(a) Layout for the three tag arrays (b) Localization results

Fig. 9. Distinguishing the three tag arrays

(a) The relative locations of the target (b) Projections of the object onto
tag array and the object the X-Y plane

Fig. 10. Localization for the centroid of the object

where n is the number of tags in the target tag array.

2) Target tag array localization: After we choose the target tag array and obtain its Z-coordinate z_c, we focus on its localization in the X-Y plane and estimate the rotation angle of the object. The antenna is adjusted to be at the same height with the target tag array according to z_c, and then we move the antenna along the X axis to compute the X and Y coordinates of each tag in the target tag array using AoA-based localization. The result is denoted as $\{(\widehat{x}_1, \widehat{y}_1), \cdots, (\widehat{x}_n, \widehat{y}_n)\}$, where $(\widehat{x}_i, \widehat{y}_i)$ is the coordinates of the ith tag. To calibrate the location of each tag, we should consider all the tags in the tag array as a whole, then the coordinates of each tag can be expressed based on the location of the tag array's center (x_c, y_c) and rotation angle α of the object according to Eq.5. That is to say, the locations of all the tags are related to (x_c, y_c) and α . Thus, the basic idea of our approach is to compute the optimal solution of (x_c, y_c) and α while referring to the fixed layout of the tag array with the AoA localization result $\{(\widehat{x}_1, \widehat{y}_1), \cdots, (\widehat{x}_n, \widehat{y}_n)\}$.

Before the optimization process, since α is in the range $[0, 2\pi]$, we can classify α into a limited range based on the position of each tag in the tag array. As mentioned before, α can be divided into four cases and each case corresponds to a unique relative position relationship of the tags in the X and Y axes. Thus, we can judge the case where α belongs to by comparing the X and Y coordinates of the 1st tag and the nth tag in the tag array. For example, as shown in Fig.5, if $\widehat{x}_1 < \widehat{x}_n$ and $\widehat{y}_1 < \widehat{y}_n$, we can then infer that $0 \leq \alpha < \pi/2$, belonging to case 1. Once the case that α belongs to is determined, the search range for the optimization process is reduced and the coordinate of the ith tag (x_i, y_i) can be expressed as a function of x_c, y_c and α according to Eq.5 as:

$$\begin{cases} x_i = x_c + p_i \cdot d \cos \beta \\ y_i = y_c + q_i \cdot d \sin \beta \\ \beta = f(\alpha) \end{cases}$$

where $|p_i|$ and $|q_i|$ can be previously determined by the tag number n of the tag array, and d is the distance between two adjacent tags.

Next, we will discuss how to find the optimal solution of x_c, y_c and α based on the AoA localization results of each tag $\{(\widehat{x}_1, \widehat{y}_1), \cdots, (\widehat{x}_n, \widehat{y}_n)\}$. Recall that the coordinate $(\widehat{x}_i, \widehat{y}_i)$ of the ith tag is computed from the point set

$$P_i = \left\{ \left(\tilde{x}_{i,1}, \cot\left(\tilde{\theta}_{i,1}\right)\right), \cdots, \left(\tilde{x}_{i,k_i}, \cot\left(\tilde{\theta}_{i,k_i}\right)\right) \right\}$$
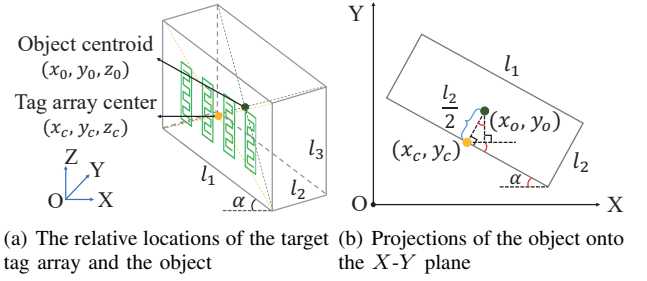
where $\tilde{\theta}_{i,j}$ represents the ith tag's angle of arrival at $\tilde{x}_{i,j}$. The linear relationship of x and $\cot\theta$ can be used to find a fitting line for P_i. Let the location of the ith tag be (x_i, y_i), then, the line can be calculated according to Eq.4 as:

$$\cot\theta_i = -\frac{1}{y_i}(x - x_i)$$

Since the coordinate of all the tags can be expressed with the tag array's center (x_c, y_c) and rotation angle α, we aims to find n fitting lines which can all be expressed with x_c, y_c and α to best fit n tags' point set $P_1, P_2, \cdots, P_n$. So, the coordinates of the *target tag array*'s center (x_c, y_c) and the object's rotation angle α can be calculated by solving the following optimization problem:

$$\arg\min_{\alpha, x_c, y_c} \sum_{i=1}^{n} \sum_{j=1}^{k_i} \left| -\frac{1}{y_i}(\tilde{x}_{i,j} - x_i) - \cot\left(\tilde{\theta}_{i,j}\right) \right|^2 \quad (8)$$

Subject to:

$$P_i = \left\{ \left(\tilde{x}_{i,1}, \cot\left(\tilde{\theta}_{i,1}\right)\right), \cdots, \left(\tilde{x}_{i,k_i}, \cot\left(\tilde{\theta}_{i,k_i}\right)\right) \right\}$$
$$x_i = x_c + p_i \cdot d \cos \beta$$
$$y_i = y_c + q_i \cdot d \sin \beta$$
$$\beta = f(\alpha)$$

In practice, the search space of x_c and y_c can be reduced when referring to $\{(\widehat{x}_1, \widehat{y}_1), \cdots, (\widehat{x}_n, \widehat{y}_n)\}$.

3) Object Localization: Notice that we finally aim to locate the object, then the centroid of the object can be regarded as our localization target. As shown in Fig.10(a), the sizes l_1, l_2, and l_3 of the object can be easily approximated, therefore, it is not difficult to infer the position of the object's centroid (x_o, y_o, z_o) from the coordinate of the target tag array's center (x_c, y_c, z_c) and the object's rotation angle α. The Z-coordinates of the object's centroid and the target tag array are equal, so, for localization in the X-Y plane, we can refer to (x_c, y_c) and α. For example, as illustrated in Fig.10(b), the 3D coordinates of the object's centroid (x_o, y_o, z_o) can be expressed as:

$$\begin{cases} x_o = x_c + l_2/2 \cdot \sin \alpha \\ y_o = y_c + l_2/2 \cdot \cos \alpha \\ z_o = z_c \end{cases} \quad (9)$$

V. PERFORMANCE EVALUATION

A. Implementation

Hardware: *3DLoc* consists of a Impinj Speedway R420 reader, a Laird S9028 RFID antenna, a motion controller, paper

boxes, and a set of Impinj E41-B tags. The reader works at the frequency band 920.625∼924.375MHz. The antenna is fixed on the motion controller which enables the linear movement along the horizontal direction and the vertical direction.

Software: We have implemented *3DLoc* in Java and we run the software in a terminal PC which is connected to the Reader with the Low-level Reader Protocol. The motion controller is programmed to move at the speed of 15cm/s for the 3D localization of the tagged objects.

B. Deployment

We conduct our experiments in the indoor environment. Fig.11 shows the experiment scene and specifies the coordinate system. The antenna is fixed on the motion controller, which supports the antenna's movement along the X axis and the Z axis. For the tagged object, we deploy three sets of tag arrays along mutually orthogonal directions on three mutually orthogonal surfaces. For each tag array, since the tag coupling effect will distort the phase value [14, 15], we ensure that two adjacent tags are deployed with opposite orientations as shown in Fig.11.

C. Micro-Benchmark

Experimental setup: The experiments are performed in two cases: free space and multipath environment. We have designed four experiments to evaluate the performance of the multipath suppression algorithm and analyze how the tag numbers and tag distances influence the localization accuracy. Since the 3D localization is expanded from the 2D plane, we first focus on the 2D localization of the tags. The antenna and the tags are all put at a height of 80cm from the ground.

Metrics: We use *error(cm)* to indicate the localization accuracy for a single tag and the tag array. Specifically for the tag array, the center of the tag array are considered as our localization target.

Determine a proper window size for multipath suppression: The slide window separates the point set for removing the outliers in the AoA-based localization. As illustrated in Fig.12, the localization error is 15cm when we set the window size to 5. The error decreases as we increase the window size from 5 to 15. However, the error increases again if we go on increasing the window size w. Therefore, we set w to 15cm as a trade-off.

With or without multipath suppression: To evaluate the performance of the multipath suppression algorithm, we localize four tags in different locations. The coordinates of the four tags are $T_1\,(0, 120)$, $T_2\,(-20, 140)$, $T_3\,(20, 140)$, and $T_4\,(-20, 160)$. As shown in Fig.13, the localization error decreases sharply when we adopt the proposed multipath suppression algorithm, i.e., the error for T_2 decreases from 45cm to 15cm.

Tag distance of the tag array vs. Localization error: Intuitively, a larger distance between the tags results in a higher localization accuracy. We localize a four-tag array in both free space and the multipath environment while changing the distance between two adjacent tags. As shown in Fig.14, in the multipath scenario, the localization error decreases

Fig. 11. Experiment scene

obviously as we increase the distance between the tags: the error drops from 15.2cm to 7.3cm as the tag distance changes from 3cm to 15cm. In free space, the localization error changes slightly when the distance changes from 3cm to 9cm and the localization errors are all around 7cm. If we further increase the distance to 12cm, the error becomes 4.3cm. In conclusion, it is more useful to increase the distance between the two adjacent tags for the tag array in the multipath environment since the localization error in free space is small.

Tag number of the tag array vs. Localization error: Generally, more tags in the tag array contributes to a lower localization error. We set the distance between the two adjacent tags to be 9cm and change the the number of tags in the tag array. As shown in Fig.15, in the multipath environment, the localization errors decrease when we increase the total number of the tags from 2 to 5: the localization error changes from 17cm to 9cm. For the free space scenario, the error for the 2-tag array is 7.1cm, thus obvious improvement cannot been seen for the localization accuracy when we increase the number of the tags in the tag array.

D. Macro-Benchmark

Experimental setup: We put the antenna on the motion controller to move along the X and Z axes to localize three tagged objects. The size of the object is $45 \times 40 \times 30$cm and it is attached with three four-tag arrays in which the distance of the two adjacent tags is 9cm. In the experiment, we place three tagged objects in different locations with different orientations.

Metrics: In the evaluation of *3DLoc*, the localization errors are calculated both for the target tag array and the object. We consider the center of the tag array and the centroid of the object as the localization target for the target tag array and the object, respectively.

In the first experiment, we evaluate *3DLoc* in comparison with the Hologram-based method. Since the orientation of the object cannot be estimated by the Hologram-based method compared with *3DLoc*, we cannot estimate location of the centroid of object. Thus We only compare the localization results of the given target tag array. As shown in Fig.16, two methods both perform well in the free space. However, in the multipath environment, the errors for *3DLoc* and the Hologram-based method are 8cm and 16.7cm respectively. So *3DLoc* outperforms the Hologram-based method significantly in the multipath environment.

In the second experiment, we place three objects in different locations and orientations, and localize them by *3DLoc* in the
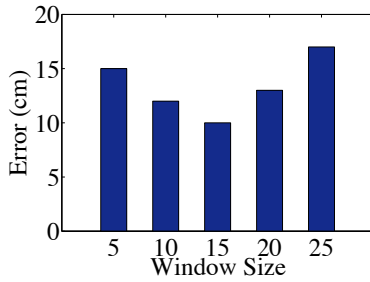
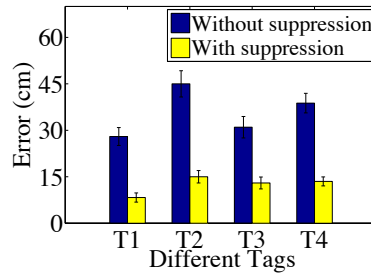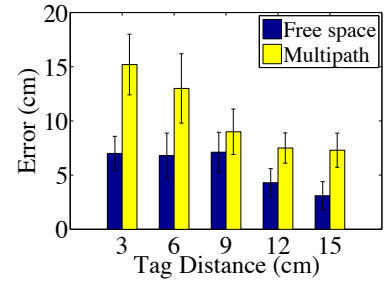Fig. 12. Window size for multipath suppression Fig. 13. The performance of multipath suppression Fig. 14. Tag distance vs. error
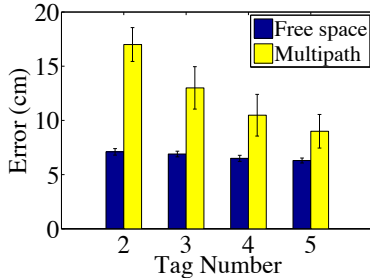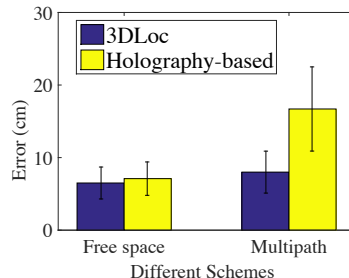

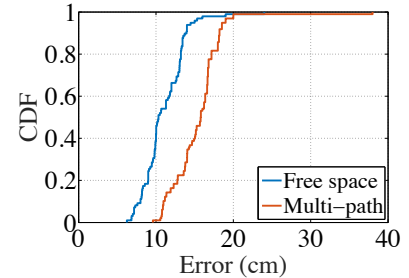Fig. 15. Tag number vs. error   Fig. 16. Scheme vs. error   Fig. 17. Error CDF

free space and the multipath environment. In the localization process, we first calculate the target tag array's 3D coordinates and object's rotation angle, and then the centroid of the object can be obtained according to Eq.9. We plot the CDF of the position error for the centroid of the object in Fig.17. The mean error of the object is 10cm and 15.3cm in the free space and the multipath environment, which is sufficient compared with the object's size $(45 \times 40 \times 30cm)$.

VI. CONCLUSION

In this paper, we propose *3DLoc* to perform 3D localization on the tagged objects using RFID tag arrays. *3DLoc* uses the AoA-based scheme to accurately estimate the tagged objects' orientations and 3D coordinates in the 3D space referring to the fixed layout of the tag array. We propose a novel algorithm to suppress the localization errors caused by the multipath effect. *3DLoc* has been implemented on a COTS RFID platform, and we have evaluated the actual performance of *3DLoc* in the real complex environment, the experiment results show that *3DLoc* can achieve a high accuracy. *3DLoc* is the first work to consider the 3D localization of tagged objects using the RFID tag arrays, and it can be applied to indoor localization systems with the severe multipath.

REFERENCES

[1] L. Shangguan, Z. Li, Z. Yang, M. Li, and Y. Liu, Otrack: Order Tracking for Luggage in Mobile RFID Systems, in *Proc. of IEEE INFOCOM*, 2013.

[2] J. Nickels, P. Knierim, B. Koenings, F. Schaub, B. Wiedersheim, S. Musiol, and M. Weber, Find My Stuff: Supporting Physical Objects Search with Relative Positioning, in *Proc. of ACM MOBIQUITOUS*, 2013.

[3] M. R. Basheer and S. Jagannathan, Localization of RFID Tags Using Stochastic Tunneling, in *IEEE TRANSACTIONS ON MOBILE COMPUTING*, vol. 12, no. 6, pp. 1225-1235, 2013.

[4] L. Yang, Y. Qi, J. Fang, X. Ding, T. Liu and M. Li, Frogeye: Perception of the slightest tag motion, in *Proc. of IEEE INFOCOM*, 2014.

[5] W. Ruan, L. Yao, Q. Sheng, N. Falkner and X. Li, TagTrack: Device-free Localization and Tracking Using Passive RFID Tags, in *Proc. of ACM MOBIQUITOUS*, 2014.

[6] J. Wang, F. Adib, R. Knepper, D. Katabi and D. Rus, RF-Compass: Robot Object Manipulation Using RFIDs, in *Proc. of ACM MOBICOM*, 2013.

[7] T. Liu, L. Yang, Q. Lin, Y. Guo and Y. Liu, Anchor-free Backscatter Positioning for RFID Tags with High Accuracy, in *Proc. of IEEE INFOCOM*, 2014.

[8] L. Xie, J. Sun, Q. Cai, C. Wang, J. Wu and S. Lu, Tell Me What I See: Recognize RFID Tagged Objects in Augmented Reality Systems, in *Proc. of ACM UBICOMP*, 2016.

[9] S. Azzouzi, M. Cremer, U. Dettmar, R. Kronberger and T. Knie, New Measurement Results for the Localization of UHF RFID Transponders Using an Angle of Arrival (AoA) approach, in *Proc. of IEEE RFID*, 2011.

[10] J. Wang and D.Katabi, Dude, where's my card?: RFID Positioning That Works with Multipath and Non-Line of Sight, in *Proc. of ACM SIGCOMM*, 2013.

[11] J. Wang, D. Vasisht and D. Katabi, RF-IDraw: Virtual Touch Screen in the Air Using RF Signals, in *Proc. of ACM SIGCOMM*, 2014.

[12] L. Yang, Y. Chen, X. Li, C. Xiao, M. Li, and Y. Liu, Tagoram: Real-time Tracking of Mobile RFID Tags to High Precision Using COTS Devices, in *Proc. of ACM MOBICOM*, 2014.

[13] L. Shangguan, and K. Jamieson, The Design and Implementation of a Mobile RFID Tag Sorting Robot, in *Proc. of ACM MOBISYS*, 2016.

[14] J. Han, Q. Chen, X. Wang, D. Ma, J. Zhao, W. Xi, Z. Jiang and Z. Wang, Twins: Device-free Object Tracking using Passive Tags, in *Proc. of IEEE INFOCOM*, 2014.

[15] L. Yang, J. Han, Y. Qi, C. Wang, T. Gu and Y. Liu, Season: Shelving interference and joint identification in large-scale rfid systems, in *Proc. of IEEE INFOCOM*, 2011.